NEUROSCIENCE
RESEARCH ARTICLE
N. J. Mills et al. / Neuroscience 390 (2018) 278–292

Aldosterone Mediated Regulation of Epithelial Sodium Channel (ENaC) Subunits in the Rat Hypothalamus

Natalie J. Mills,[1] Kaustubh Sharma[1] Masudul Haque Meagan Moore and Ryoichi Teruyama*

Department of Biological Sciences, Louisiana State University, LA 70803, USA

Abstract—Current evidence suggests that the epithelial Na^+ channel (ENaC) in the brain plays a significant role in the development of hypertension. ENaC is present in vasopressin (VP) neurons in the hypothalamus, suggesting that ENaC in VP neurons is involved in the regulation of blood pressure. Our recent study demonstrated that high dietary salt intake caused an increase in the expression and activity of ENaC that were responsible for the more depolarized basal membrane potential in VP neurons. A known regulator of ENaC expression, the mineralocorticoid receptor (MR), is present in VP neurons, suggesting that ENaC expression in VP neurons is regulated by aldosterone. In this study, the effects of aldosterone and corticosterone on ENaC were examined in acute hypothalamic slices. Real-time PCR and Western blot analysis showed that aldosterone and corticosterone treatment resulted in a significant increase in the expression of γENaC, but not α- or βENaC, and that this expression was attenuated by MR and glucocorticoid receptor (GR) antagonists. Moreover, chromatin immunoprecipitation demonstrated that the aldosterone-MR complex directly interacts with the promoter region of the γENaC gene. However, the treatment with aldosterone did not cause subcellular translocation of ENaC toward the plasma membrane nor an increase in ENaC Na^+-leak current. These results indicate that expression of γENaC in VP neurons is induced by aldosterone and corticosterone through their MR and GR, respectively; however, aldosterone or corticosterone alone is not sufficient enough to increase ENaC current when they are applied to hypothalamic slices *in vitro*.

Key words: mineralocorticoid receptor, glucocorticoid receptor, vasopressin, supraoptic nucleus.

INTRODUCTION

Vasopressin (VP) is synthesized in magnocellular neurons located in both the paraventricular (PVN) and the supraoptic (SON) nuclei of the hypothalamus and is released from the neurohypophysis into the general circulation. VP neurons increase VP secretion in response to hyperosmolality (Brimble and Dyball, 1977), hypovolemia (Harris et al., 1975) and hypotension (Khanna et al., 1994) to produce antidiuretic and pressor effects. The release of VP also occurs from the soma and dendrites of VP neurons in the PVN to increase the activity of parvocellular neurons within the PVN that project to the rostral ventrolateral medulla (Son and Stern, 2011). This action affects sympathetic outflow and blood pressure (Dampney, 1994). VP neurons thus play a pivotal role in coordinating neuroendocrine and autonomic responses to maintain cardiovascular homeostasis. Because the release of VP depends largely on the pattern of neuronal activity of their synthesizing neurons (Poulain and Wakerley, 1982; Cazalis et al., 1985), factors modulating neuronal activity of these neurons are of great interest.

The non-voltage-dependent and amiloride-sensitive epithelial Na^+ channel (ENaC) is a member of the degenerin/epithelial sodium channel (Deg/ENaC) superfamily and is composed of three subunits (α, β, and γ) that form a highly selective Na^+ channel (Canessa et al., 1994). ENaC are present in aldosterone-sensitive epithelia that are responsible for trans-epithelial Na^+ transport, such as in epithelial cells that line the distal part of the renal tubule, the distal colon, the duct of several exocrine glands, and the lung. ENaC was also demonstrated in various structures in the brain, namely the SON, PVN, subfornical organ, choroid plexus, and ependyma of the anteroventral third ventricle (Amin et al., 2005). The function of ENaC in the brain was studied in the choroid plexus and VP neurons in the SON. In the choroid plexus, ENaC plays a role in Na^+-transport between blood and cerebrospinal fluid (CSF), and thereby in regulation of CSF $[Na^+]$ (Amin et al., 2009). In VP neurons, ENaC modulates

*Corresponding author. Address: Louisiana State University, 202 Life Sciences Building, Baton Rouge LA70803, USA.
E-mail address: rteruyama@lsu.edu (R. Teruyama).
[1] N.J. Mills and K. Sharma contributed equally to this manuscript.
Abbreviations: ACSF, artificial cerebrospinal fluid; Deg, degenerin; ENaC, epithelial sodium channel; GR, glucocorticoid receptor; MR, mineralocorticoid receptor; PVN, paraventricular nucleus; SON, supraoptic nucleus; VP, vasopressin.

https://doi.org/10.1016/j.neuroscience.2018.08.031
0306-4522/

the membrane potential by mediating a Na^+ leak current (Teruyama et al., 2012).

Several physiological studies showed that central administration of the ENaC blocker, amiloride or its analog benzamil, attenuates sympathetic activity and hypertension in several animal models of hypertension (Gomez-Sanchez and Gomez-Sanchez, 1994, 1995; Nishimura et al., 1998; Keep et al., 1999; Nishimura et al., 1999; Wang and Leenen, 2002; Wang et al., 2003) and heart-failure (Ito et al., 2015). Because the amounts of central administration of amiloride or benzamil used in these studies were too small to be effective if they were administered in the general circulation, the effects of amiloride or benzamil on sympathetic activity and hypertension were most likely mediated by ENaC in the brain. While these studies provide little information regarding the locations of ENaC action(s) in the brain, these studies indicate that abnormally regulated ENaC in the brain plays a significant role in the development of hypertension.

Our recent studies showed that animals that consumed high dietary salt displayed an enhanced ENaC current, which resulted in further depolarization of the basal membrane potential of VP neurons (Sharma et al., 2017). These findings indicate that high dietary salt intake enhances the expression and activity of ENaC, which in turn, augments synaptic drive during hormonal demand by depolarizing the basal membrane potential closer to the action potential threshold. Activation of ENaC, therefore, is a powerful means to modulate hormone secretion according to physiological demands. Furthermore, considering the role of VP in the cardiovascular homeostasis, ENaC in VP neurons may have a major role in the regulation of blood pressure; however, the mechanism underlying the regulation of ENaC activity in VP neurons remains mostly unknown.

ENaC expression in epithelia is primarily regulated by the mineralocorticoid, aldosterone, via the mineralocorticoid receptor (MR) (Renard et al., 1995; Escoubet et al., 1997; Stokes and Sigmund, 1998; Masilamani et al., 1999; MacDonald et al., 2000). The MR was also found in various parts of the brain, namely the choroid plexus, ependyma, neurons in the SON and PVN, the nucleus tractus solitarius, and in the subfornical organ (van Eekelen et al., 1991; Amin et al., 2005; Han et al., 2005; Geerling and Loewy, 2009; Teruyama et al., 2012). Of these MR-expressing structures, colocalization of the MR and ENaC was found in magnocellular neurons of the SON and PVN, choroid plexus, and ependyma (van Eekelen et al., 1991; Amin et al., 2005; Han et al., 2005; Geerling and Loewy, 2009; Teruyama et al., 2012; Haque et al., 2015). The colocalization of the MR and ENaC in VP neurons (Teruyama et al., 2012; Haque et al., 2015) suggests that ENaC in VP neurons is also regulated by aldosterone. The present study that used acutely prepared hypothalamic slices incubated with aldosterone, was conducted to examine the effects of aldosterone on the expression and activity of ENaC in VP neurons. This *in vitro* approach allowed us to evaluate the effect of aldosterone on ENaC in VP neurons more directly without the context of whole animal physiology.

EXPERIMENTAL PROCEDURES

Animals

Male Wistar rats (Harlan Laboratories, Indianapolis, IN) weighing between 260 and 300 g were used in the present investigation. Rats were housed on a 12:12-h light–dark cycle and were allowed standard chow and water *ad libitum*. All protocols were carried out in accordance with the National Institute of Health Guide for the Care and Use of Laboratory Animals and were approved by the Institutional Animal Care and Use Committees of Louisiana State University.

Acute hypothalamic slice preparation

Rats were deeply anesthetized with Ketamine–Xylazine (9:1, 100 mg/kg i.p.) and perfused through the heart with cold artificial cerebral spinal fluid (ACSF), in which NaCl was replaced by equiosmolar sucrose (containing, in mM, 210 Sucrose, 3 KCl, 2.0 $CaCl_2$, 1.3 $MgCl_2$, 1.24 NaH_2PO_4, 25 $NaHCO_3$, 0.2 ascorbic acid, and 10 D-glucose; pH 7.4). The brain of each rat was removed and three coronal slices (500 μm), containing the entirety of the SON and PVN, were collected using a vibrating microtome (Leica VT1200; Leica, Mannheim, Germany). Other brain areas that are known to express ENaC, namely the vascular organ of lamina terminalis (OVLT) (Miller and Loewy, 2013), area postrema (Miller et al., 2013), and subfornical organ (SFO) (Wang et al., 2016), were not included. Slices were divided into two equal halves along the midline at the third ventricle using microdissection scissors. Slice halves from the same side were placed in the control group, while the other halves were placed in the treatment group.

In vitro incubation with corticosteroids

The hypothalamic slices were incubated on a plastic tray that consisted of wells with nylon mesh bottom to hold individual slices in a glass beaker that was filled with 200 ml ACSF (in mM: 125 NaCl, 2.5 KCl, 1 $MgSO_4$, 1.25 NaH_2PO_4, 26 $NaHCO_3$, 10 D-glucose, 2 $CaCl_2$, 0.4 Ascorbic acid, pH of 7.3–7.4) with normal physiological osmolality and [Na^+] (~295 mOsm/kg and 151.24 mM, respectively). The normal physiological osmolality of ACSF was chosen to avoid possible effects of higher osmolality on ENaC expression, since intracerebroventricular (ICV) infusion of Na^+-rich ACSF caused an increase in hypothalamic aldosterone concentration in rats (Huang et al., 2008) and vasopressin neurons are directly osmosensitive (Oliet and Bourque, 1993). The slices were continuously oxygenated with 95% O_2/5% CO_2 gas and maintained at 34 °C. The incubation trays were placed at approximately half the depth of the beaker to ensure that the slices were completely immersed throughout the experiment. Slices were incubated for 6 h with aldosterone, corticosterone, or vehicle. The incubation time of 6 h was chosen, because the pilot study showed 6 h is the minimum duration that produced significant changes in the amount of γENaC mRNA. In addition, a longer than 6-h incubation time did not allow us to conduct several-hour-long electrophysiological

experiments before the brain slices started to deteriorate. In some experiments, slices were incubated for 30 min with the antagonist for the MR or glucocorticoid receptor (GR) to block MR and GR prior to aldosterone or corticosterone application, respectively. Following incubation, slices were trimmed along the dorsal portion of the third ventricle lateral to the optic chiasm to minimize tissue that did not contain the PVN and SON and to exclude the choroid plexus that is known to express ENaC subunits (Amin et al., 2005). Trimmed slices were placed in RNA-Later (Qiagen, CA) and stored at −20 °C for later processing. Additional hypothalamic slices were fixed in 4% paraformaldehyde with 0.1% picric acid in 0.15 M sodium phosphate buffer (pH 7.2–7.4) and processed for immunocytochemistry.

Corticosteroids and antagonists

Aldosterone and corticosterone were purchased from Sigma–Aldrich (St. Louis, MO). Antagonists for MR and glucocorticoid receptors (GR) were RU-28318 (Tocris Bioscience, Ellisville, MO) and RU-486 (Sigma–Aldrich, St. Louis, MO), respectively. All compounds were dissolved into dimethyl sulfoxide (DMSO) to make stock solutions and were further diluted in ACSF to reach the final concentration. RU-28318 used for incubations was 2.5 μM, whereas that of RU-486 was 5 μM. The concentration of these competitive antagonists was determined based on published reports that RU-28318 and RU-486 competitively bind to the receptor with an affinity similar to that of the mineralocorticoid (Janiak and Brody, 1988) and glucocorticoid (Schreiber et al., 1983). The final concentration of DMSO in ACSF was 0.05% when aldosterone or corticosterone was applied and 0.1% when MR or GR antagonists were applied in addition to aldosterone or corticosterone.

Real-time PCR

Total RNA was isolated using TriReagent (Sigma–Aldrich, St Louis, MO) according to the manufacturer's instructions, and tissue was homogenized using a tissue lyser (Qiagen, Valencia, CA). Lysate was then treated with chloroform (ThermoFisher Scientific, Waltham, MA) and centrifuged at 12,000 rpm for 15 min. Total RNA was precipitated from the aqueous stage using isopropyl alcohol, and then washed with ethanol. Precipitate was suspended in 20 μl RNase-free water. The concentration and quality of the isolated RNA were assessed using a spectrophotometer (NanoDrop 1000, ThermoFisher Scientific, Waltham, MA). Isolated mRNA was reverse transcribed to cDNA using oligo dT and M-MLV reverse transcriptase (Sigma–Aldrich, St. Luis, MO) and used in real-time RT–PCR analysis. The ABI ViiA-7 sequence detection system (ABI Applied Biosystem, Grand Island, NY) was used in conjunction with the SYBR Select Master Mix (ABI Applied Biosystem, Grand Island, NY). All samples were measured in triplicate and the two closest cycle threshold (Ct) values were averaged for each sample.

The effect of the treatments was examined via the relative changes of the specific target genes, which were calculated using the comparative cycle threshold method. For each sample, the average Ct value of the target gene was subtracted by the housekeeping (Cyclophilin B) gene to obtain the ΔCt value. The ΔCt values of the designated control group were averaged and subtracted from each sample to generate the ΔΔCt value. Relative change was then calculated for each sample using the formula $2^{-\Delta\Delta Ct}$. All results are shown as relative change in comparison to the control. The paired Student's t test was used for comparison between treatment groups. Differences were considered to be statistically significant at $p < 0.05$.

Primers of selected genes were designed using Primer 3 software (Whitehead Institute for Biomedical Research) and purchased from Sigma–Aldrich (St. Louis, MO). All primer sequences were blasted on the National Center for Biotechnology Information database to determine specificity of targeted gene. The sequences of the primer used are listed in Table 1.

Semiquantitative immunoblotting

Total protein lysate samples were collected from above-mentioned hypothalamic slice preparation. The hypothalamic slices were incubated for 6 h with 2.5 μM aldosterone or vehicle, and were rinsed with cold PBS and placed in microcentrifuge tubes containing 250 μl of chilled complete lysis buffer. Lysis buffer was made fresh before each experiment. Complete buffer contained: RIPA buffer (50 mM NaCl, 1.0% IGEPAL® CA-630, 0.5% sodium deoxycholate, 0.1% SDS, 50 mM Tris, pH 8.0; Sigma–Aldrich, St. Louis, MO), protease inhibitors (ProteoGuard™ EDTA-free protease inhibitor cocktail; Takara Clontech, Mountain View, CA), 1 mM EGTA, 1 mM EDTA, and 1 mM DTT. Samples were briefly homogenized utilizing an electric tissue lyser (Qiagen, Valencia, CA) and allowed to stand on ice for 10 min. Lysed samples were centrifuged for 20 min at 12,000 rpm at 4 °C. The pellet was discarded and the clear supernatant (total lysate) was transferred to a clean tube to be stored at −20 °C for later processing.

After protein concentration was determined (BCA kit; Pierce Chemical Co., Rockford, Illinois, USA), samples (15–20 μg of protein) were denatured by heating in 1x Laemmli buffer (Bio-Rad) for 5 min at 95 °C. Samples were resolved in a 4–15% SDS–PAGE (Mini PROTEAN Precast Gels, Bio-Rad) gradient gel in Tris-glycine buffer (25 mM, 192 mM glycine, 0.1% SDS, pH 8.3; Bio-Rad) and transferred to a PVDF membrane (Bio-Rad, Hercules, CA) under wet conditions (50 V for 2 h at 4 °C). To determine a successful transfer, the membrane was stained with Ponceau S solution (Sigma–Aldrich, St. Louis, MO) for approximately 1 min. The membrane was destained with 0.1 M NaOH for 30 s followed by quick TBST wash (TBS-Tween; 50 mM Tris base, 200 mM NaCl, 0.05% Tween 20). The membrane was blocked with 5% non-fat buffer (NFM; Bio-Rad, Hercules, CA) for 1 h at room temp, and incubated overnight at 4 °C with the selected primary antibody dissolved in 5% NFM buffer. A final concentration for all ENaC primary antibodies was 1 μg/ml. Glyceraldehyde 3-phosphate dehydrogenase (GAPDH; Abcam,

Table 1. Primer sequences used to detect genes of interest.

Gene		Primer Sequence	Amplicon Size
αENaC	F	5′-CCCAAGGGAGTTGAGTTCTG-3′	76 bp
	R	5′-AGGCGCCCTGCAGTTTAT-3′	
βENaC	F	5′-GGACCAGAGCTAAATATCACC-3′	78 bp
	R	5′-CGGTAGTTGAACTCTTGGAAGTAGA-3′	
γENaC	F	5′-CCAGTACAGCCAGCCTCTG-3	91 bp
	R	5′-CTGGTACAACTGGTAGTAGCAATACAT-3′	
VP	F	5′-CACCTATGCTCGCCATGAT-3′	299 bp
	R	5′-GCTTCCGCAAGGCTTCT-3′	

Cambridge, MA) primary antibody was used as a load control with a final concentration of 0.125 μg/ml. The next day, the membrane was washed three times for 10 min each with TBST and incubated with the horseradish peroxidase-conjugated (HRP) secondary antibody against the respective host species (1:10,000, Goat-anti Rabbit – HRP; 1:10;000, Goat-anti Mouse, Bio-Rad) dissolved in 5% NFM buffer at room temp for 2 h followed by six TBST washes for 10 min each. Protein bands were detected through chemiluminescence reagents (Clarity™ Western ECl Substrate Kit; Bio-Rad, Hercules, CA) and imaged utilizing a gel imaging system (ChemiDoc™ XRS + ; Bio-Rad, Hercules, CA). Densitometric measurements were obtained through ImageJ (NIH, Bethesda, MD).

Chromatin immunoprecipitation (ChIP) and qPCR analyses

The rats ($n = 19$) were deeply anesthetized with Ketamine:Xylazine (9:1; 100 mg/kg; i.p.) and transcardially perfused with an artificial cerebrospinal fluid (ACSF) in which NaCl was replaced by equiosmolar sucrose (in mM: 210 Sucrose, 3 KCl, 2 $CaCl_2$, 1.3 $MgCl_2$, 1.24 NaH_2PO_4, 25 $NaHCO_3$, 0.2 ascorbic acid, and 10 D-glucose; pH 7.4). The brains were removed and a hypothalamic block (4.5 mm: 0.4gm) containing the SON and PVN was made. Kidneys were also removed and blocked to be of equal weight as the brain. The blocked tissues were ground and homogenized in 2 ml sodium phosphate-buffered saline (PBS; pH 7.2) containing 20 μl protease inhibitor (635673, Clontech, Mountain View, CA). The homogenized samples were first cross-linked with 1% formaldehyde for 20 min at 37 °C, and then lysed in SDS lysis buffer (1% SDS, 10 mM EDTA, 50 mM Tris–HCl; pH 8.1) containing a protease inhibitor. The released nuclei were fractioned with sonication to obtain a pool of DNA fragments of 300–500 bp in length. The sonicated samples were divided into 3 individual aliquots. 60 μl of the protein A/G plus agarose beads (sc-2003, Santa Cruz Biotechnology, Dallas, TX) were added to two tubes and incubated for 2 h at 4 °C with gentle agitation to preclear the lysates. One tube containing the lysate was used as the input control. The samples were centrifuged at 2000 rpm at 4 °C for 5 min, and one of the two subsequent supernatants was used for immunoprecipitation. Four different anti-MR monoclonal antibodies (rMR1-18 1D5, MRN2 2B7, MRN3 3F10, and rMR365 4D6) were obtained from the Developmental Studies Hybridoma Bank (Iowa City, IA). The supernatants were incubated with a cocktail of the anti-MR antibodies at equal ratio (2.5 μg) for overnight at 4 °C with gentle agitation. After incubation with the antibodies, 120 μl of the protein A/G agarose beads were added to both tubes (with Ab and without Ab) and incubated overnight at 4 °C. Subsequently, the samples were centrifuged at 1000 rpm at 4 °C for 5 min to remove the supernatants and the remaining beads were washed five times in wash buffers. The proteins were eluted using an elution buffer containing 1% SDS and 0.1 M $NaHCO_3$. The protein–DNA crosslinks were reversed by heating at 65 °C overnight with gentle agitation. The DNA was recovered by phenol/chloroform extraction, precipitated with ethanol, and dissolved in 25 μl TE buffer (pH 8.0). Input control, Ab, and no Ab samples (2 μl each) were subjected to PCR with JumpStart REDTaq DNA polymerase (D0563, Sigma–Aldrich, St. Louis, MO) to detect the MR-binding sites in the promoter region in *Scnn1g*. The primer set (Forward 5′-GAAGGGTGAGATGGATTGGA-3′ and Reverse 5′-GTAGGGGAAAGGGGGTAACA-3′, chr1: 191706400–191706675, 276 bp) was specifically designed based on a previous study (Lombès et al., 1993). The following PCR conditions were used: 95 °C for 90 s, 45 repetitions of the following cycles 95 °C for 30 s, 60 °C for 10 s, 72 °C for 60 s, and final extension at 72 °C for 5 min. The PCR products from the input DNA, negative control (no Ab) and MR ChIP were separated by agarose gel electrophoresis and visualized with ethidium bromide. For quantitative PCR (qPCR) analysis, the total DNA concentrations of the samples were measured using Nanodrop 2000 (Thermo Fisher Scientific, Waltham, MA) and normalized so that equal amounts of DNA were amplified. The normalized product (2 μl) was used for PCR with SYBR Select Master Mix (4472897, ABI Applied Biosystems, Foster City, CA). The following PCR conditions were used: 95 °C for 90 s, 40 repetitions of the following cycles 95 °C for 30 s, 60 °C for 60 s, and final extension at 72 °C for 5 min. Results are reported as a percent change compared to the input control.

Immunocytochemistry

Hypothalamic slices from six animals were processed concurrently under the same conditions for immunocytochemical localization of ENaC subunits. The

500-μm-thick hypothalamic slices were cryoprotected by immersing in 50% glycerol in PBS for ~5 min before mounting on a freezing microtome (SM2010R; Leica, Mannheim, Germany) and sectioned at 40 μm. Slices were incubated with 5% normal goat serum in PBS containing 0.5% Triton X-100 (PBST) for 30 min at room temperature followed by the primary antibodies directed against αENaC, βENaC, or γENaC at dilutions of 1:2000, 1:500, and 1:4000, respectively at 4 °C with continuous gentle agitation for overnight. The rabbit antibodies against the ENaC subunits were a generous gift from Dr. Mark A. Knepper (National Institutes of Health, Bethesda, MD), and the characterizations of these antibodies were previously described in great detail (Masilamani et al., 1999). The hypothalamic slices were incubated with biotinylated goat-anti-rabbit IgG (1:500 in PBST; Vector, Burlingame, CA) for 2 h and with ABC complex (1:500 in PBST, Vector, Burlingame, CA) for 1 h. Subsequently, slices were incubated with diaminobenzidine (DAB; Vector, Burlingame, CA) to visualize the immunoreactivity. Slices were washed in PBST (3x5 min each) between each step. Finally, slices were mounted on subbed slides, air-dried overnight, dehydrated in a series of alcohols, cleared in xylene, and coverslipped with Permount (Fisher Scientific, Waltham, MA) mounting medium. The hypothalamic slices containing the SON and PVN were digitally photomicrographed in 12-bit intensity levels using a microscope (Nikon Eclipse 80i, Tokyo, Japan) equipped with a digital camera (Nikon DS-QiMc, Tokyo, Japan).

For fluorescent confocal microscopy, the brain slices were incubated with a secondary antibody (goat anti-rabbit) conjugated with DyLight 594 (Jackson ImmunoResearch, West Grove, PA) for 4 h at room temperature. The hypothalamic slices were examined with a confocal microscope (Leica TCS SP8, Mannheim, Germany) using a 63X/1.4n.a. oil immersion objective lens. Confocal images (1024x1024; 0.232 μm/pixel) were acquired at the optical section thickness of 1 μm.

Electrophysiology

Brain slices were obtained as described in *Acute hypothalamic slice preparation* and incubated with aldosterone or vehicle for 6 h prior to the electrophysiological experiments. Whole-cell currents were recorded digitally at 20 kHz and filtered at 5 kHz with a Digidata 1440A and an Axopatch 700B (*Molecular Devices*, Foster City, CA) amplifier in conjunction with PClamp 10 software (*Molecular Devices*, Foster City, CA). Magnocellular neurons in the SON were visually identified with a microscope (Olympus BX50WI, Tokyo, Japan) equipped with a 40× water immersion lens (0.8n.a., Olympus, Tokyo, Japan). Recordings were taken using borosilicate electrodes (4–8 MΩ resistance) produced with a horizontal electrode puller (Model P-1000 Micropipette puller, Sutter Instruments, Novato, CA). The intracellular solution (in mM: 140 K-Gluconate, 1 $MgCl_2$, 10 HEPES, 10 $CaCl_2$, 2 ATP (Mg^{2+}), and 0.4 GTP (Na^+), 11 EGTA, pH was adjusted to 7.25 with KOH, osmolality of 285 mOsm/kg H2O) contained 0.2% biocytin (Sigma–Aldrich, St. Louis, MO) to identify the cell type of the patched cell (Teruyama and Armstrong, 2005, 2007). The extracellular solution (ACSF described above) was saturated with 95% O_2/5% CO_2, and warmed to 33–34 °C during the recordings. ACSF contained picrotoxin and DNQX (100 and 10 μM, respectively) to suppress the synaptic activity. The ENaC current was estimated from the benzamil-sensitive current that was obtained from the difference in the steady-state currents before and after the application of benzamil (2 μM). Amiloride and its derivative benzamil are known potent blockers of the degenerin/epithelial sodium channel superfamily of ion channels and the Na^+/H^+ exchanger (NHE) and the Na^+/Ca^{2+} exchanger (NCX); however, benzamil at the dosage used in this study (2 μM) is reasonably specific for ENaC as compared to the NHE and NCX (Kleyman and Cragoe, 1988).

Statistics

Real-time PCR data were analyzed with the paired Student's *t* test for comparison between treatment groups and control. For semi-quantitative immunoblotting, densitometric measurements of bands were analyzed as comparison between control and aldosterone values for individual animals. Differences were considered to be statistically significant at $p < 0.05$. Box and whisker plots were used to represent numerical data: the mean and median are represented by an open circle and a line, respectively; the box extends to the quartiles of the data points; the whiskers extend to the farthest data points.

RESULTS

Dose–response relationship of aldosterone and ENaC subunit expression in the hypothalamus

Dose–response relationships of aldosterone and ENaC subunit gene expression were assessed by changes in the relative amount of mRNA for each of the subunits in response to incubation for 6 h with aldosterone at concentration of 0.1 ($n = 6$), 0.5 ($n = 15$), 2.5 ($n = 12$), and 12.5 ($n = 6$) μM. The expression of αENaC and βENaC did not change significantly in response to aldosterone at any concentration tested; however, the expression of γENaC was significantly higher on the side of hypothalamus that was incubated with aldosterone at 2.5 ($p = 0.003$) and 12.5 ($p = 0.038$) μM compared to the side of the hypothalamus incubated with vehicle only. When the responses were plotted on log concentration of aldosterone, only the expression of γENaC showed a graded dose–response (Fig. 1). Because the minimum concentration of aldosterone required to induce a significant level of γENaC expression within 6 h was 2.5 μM; subsequent experiments were conducted using 2.5 μM aldosterone.

Aldosterone induces γENaC expression via the MR in the hypothalamus

The effect of aldosterone on the expressions of α-, β-, and γENaC subunits in the hypothalamus was assessed by

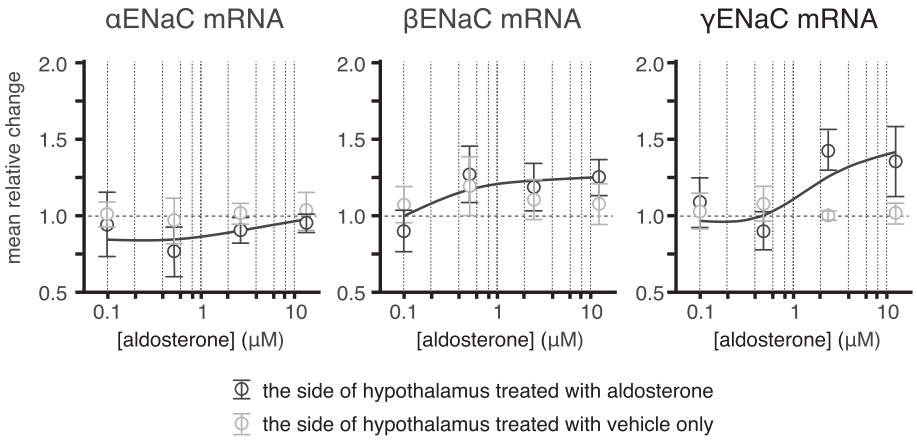

Fig. 1. Dose–response relationship of aldosterone and the expression of ENaC subunits. Semi-log plots of changes in the relative amount of ENaC subunit mRNA in the hypothalamus in response to different concentration of aldosterone. The expression of αENaC and βENaC did not change significantly at any concentration tested; however, the expression of γENaC was significantly higher on the side of hypothalamus that were incubated with aldosterone at concentrations higher than 2.5 μM compared to the side of the hypothalamus incubated with vehicle only. Data are shown as mean ± SE.

changes in the relative amount of mRNA for each of the subunits. A significantly higher expression of γENaC was observed on the side of the hypothalamic slice that was incubated with aldosterone compared to the side incubated with vehicle only (Fig. 2A). In contrast to γENaC mRNA, no detectable effects of aldosterone on the amount of αENaC or βENaC mRNAs were observed. To determine if the effect of aldosterone on the expression γENaC was mediated by the MR, one side of the hypothalamic slices was treated with a selective MR antagonist, RU-28318, prior to the application of aldosterone. The relative amount of γENaC mRNA was significantly lower on the side of the hypothalamic slices pretreated with the MR antagonist compared to the aldosterone-only treated side suggesting that the MR antagonist prevented the aldosterone-induced γENaC expression (Fig. 2B). There was no detectable difference in the relative amounts of αENaC and βENaC subunit mRNAs between the RU28318 pretreated and non-treated groups (Fig. 2B). In addition, the treatment with RU28318 alone did not affect the relative amounts of αENaC, βENaC, or γENaC subunit mRNAs (Fig. 2C).

Semi-quantitative immunoblotting was also performed to assess whether the abundance of ENaC subunit proteins changed in response to aldosterone. A distinct band at the predicted molecular weight of 87 kDa and 85 kDa in protein extract from the hypothalamus was detected by αENaC and γENaC antibodies, respectively (Fig. 3A). No detectable band was labeled by the βENaC antibody in the protein extracted from the hypothalamus (Fig. 3A), although a band at the predicted molecular weight of 88 kDa was labeled by the βENaC antibody in the protein extract from the kidney cortex (data not shown). The abundance of γENaC protein increased significantly on the side of hypothalamic slice that was incubated with aldosterone; however, the abundance of αENaC protein was unchanged (Fig. 3B).

Furthermore, Chromatin Immunoprecipitation (ChIP) was performed to assess whether the aldosterone–MR complex directly regulated the expression of the γENaC gene (*Scnn1g*). MR antibodies were used to precipitate fractions of DNA containing the MR. Real-time PCR with a specific primer set detected the promoter region of *Scnn1g* in the MR-immunoprecipitated DNA fractions from the hypothalamic block containing the SON and PVN (Fig. 4).

Corticosterone induces γENaC expression through the GR in the hypothalamus

The effect of corticosterone on the expressions of the α, β, and γ ENaC subunits in the hypothalamus was also assessed by determining the relative amount of mRNA for each of the subunits. Incubation with corticosterone caused a significantly higher γENaC subunit expression on that side of hypothalamic slice; however, no detectable effects were observed in the expression of the αENaC and βENaC subunits (Fig. 5A).

Because the MR has a similar binding affinity for both mineralocorticoids and glucocorticoids (Funder, 1995), experiments were performed to determine if the MR mediated the effect of corticosterone on γENaC expression. One side of the hypothalamic slices was pre-treated with the MR-antagonist, RU-28318, prior to the application of corticosterone, while the other side was treated with corticosterone only. No significant difference was detected in the relative amounts of mRNAs for all ENaC subunits between the corticosterone-only treated side of the hypothalamic slices and those treated with the MR antagonist and corticosterone (Fig. 5B), indicating pretreatment with RU-28318 failed to block an increase in γENaC mRNA by corticosterone in hypothalamic slices.

Because the MR antagonist was unable to attenuate the effects of corticosterone on γENaC expression, it was likely that corticosterone bound to the GR to induce γENaC expression in the hypothalamus. To test this hypothesis, one side of the hypothalamic slices was pre-treated with RU-486, a selective GR antagonist, prior to the application of corticosterone, while the other side was treated with corticosterone only. The relative amount of γENaC mRNA was significantly lower on the side of hypothalamic slices treated with RU486 compared to those treated with corticosterone only; also, there were no detectable differences in αENaC or βENaC expression between the treatment groups (Fig. 5C). In addition, the treatment with RU486 alone did not affect the relative amounts of αENaC, βENaC, or γENaC subunit mRNAs (Fig. 5D). Taken together, these results indicate that GR antagonism was able to

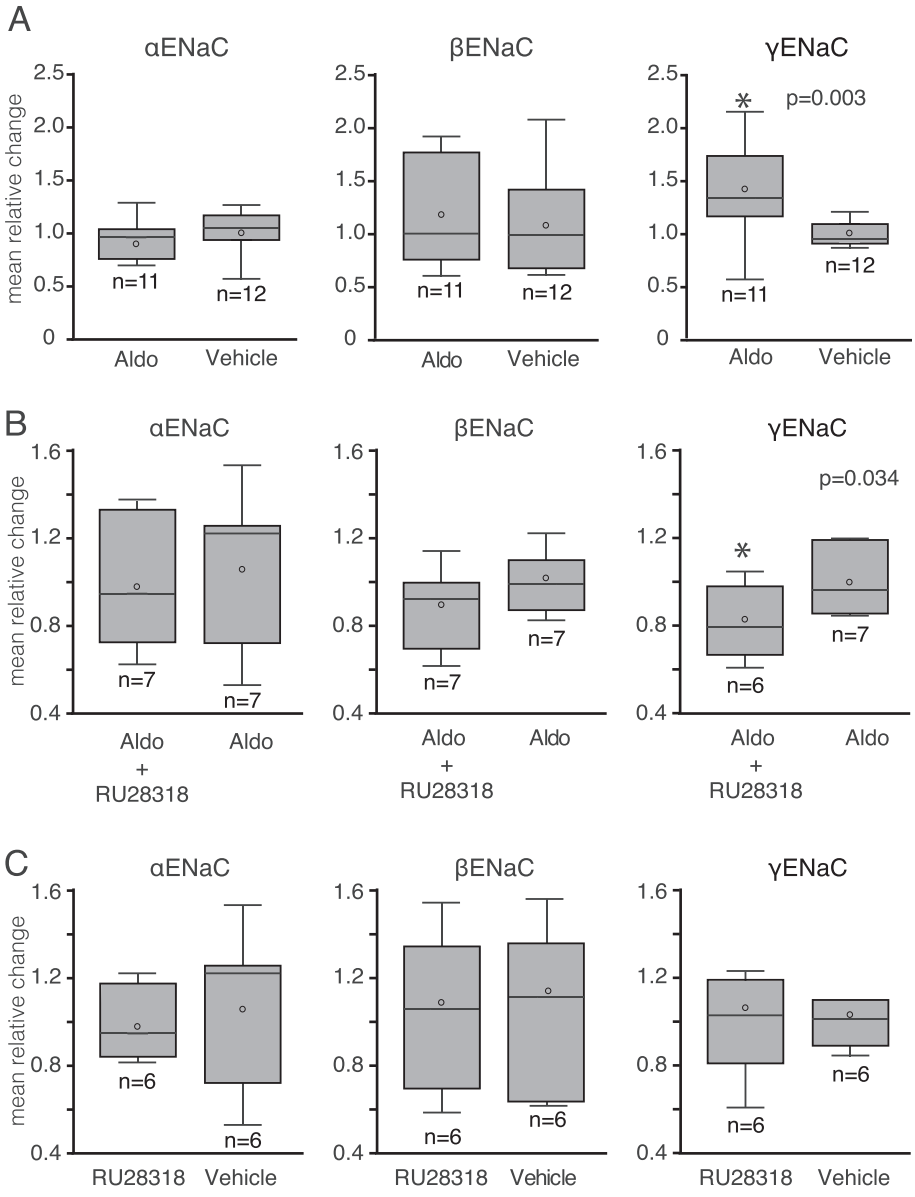

Fig. 2. The effect of aldosterone on ENaC subunit expression in hypothalamic slices. (A) No significant difference in the relative amounts of αENaC and βENaC subunit mRNAs was identified between the aldosterone-incubated and control side of hypothalamic slices; however, only the aldosterone-incubated side had a significantly greater amount of γENaC subunit mRNA ($^{*}p < 0.003$). B. No significant differences in αENaC and βENaC subunit expression occurred between the sides of the hypothalamic slices that were pre-incubated with and without RU-28318, respectively; however, the side of the hypothalamic slices that was not pre-incubated with RU-28318 had a significantly higher γENaC subunit expression compared to the side pre-incubated with MR antagonist, RU-28318 ($^{**}p < 0.034$). C. No significant differences in αENaC, βENaC, or γENaC subunit expression observed between the sides of the hypothalamic slices that were incubated with and without RU-28318.

attenuate the effect of corticosterone on γENaC expression.

Subcellular distribution of ENaC subunit immunoreactivity

In the region of the hypothalamus used for semi-quantification of the ENaC subunit mRNAs and proteins in the present study, immunoreactivity of the ENaC subunits was exclusively found in magnocellular neurons in the SON and PVN (Fig. 6 A&B). No immunoreactivity of ENaC subunits was observed in the ependymal cell layers or in the endothelium of blood vessels. Because our recent study showed that the αENaC labeling was distinctively concentrated near the plasma membrane in neurons from animals that were fed a high-salt diet (Sharma et al., 2017), the effect of aldosterone on the subcellular distribution of ENaC subunits immunoreactivity was also examined. Intense αENaC immunoreactivity that was moderately concentrated toward the plasma membrane was observed in most of the magnocellular neurons; however, no noticeable differences in subcellular distribution of ENaC immunoreactivity occurred between control and aldosterone-treated hypothalamic slices from six different animals (Fig. 6C). Weak, but prominent, immunoreactivity of βENaC was observed in the cytoplasm of magnocellular neurons (Fig. 6C). In contrast to βENaC immunoreactivity, γENaC immunoreactivity was intense and fully filled the cytoplasm of magnocellular neurons (Fig. 6C).

Aldosterone did not change expression of vasopressin

In the kidney, VP promotes Na^+ reabsorption by inducing the expression of β- and γ-ENaC subunits (Djelidi et al., 1997; Ecelbarger et al., 2000; Nicco et al., 2001; Sauter et al., 2006) and the translocation of intracellular pools of pre-existing ENaC subunits to the apical membrane of the principal cells in the collecting duct (Schafer and Hawk, 1992). The effect of aldosterone and corticosterone on the expression of VP was assessed to evaluate possible effect of corticosteroid-induced VP on ENaC activity. Semiquantitative PCR found that neither incubation with aldosterone nor corticosterone produced changes in expression of VP in the hypothalamic slices (Fig. 7).

Effect of aldosterone on the benzamil-sensitive current

Of forty-five recorded VP neurons from 21 rats, 25 neurons were from the aldosterone-treated side, and 20 neurons were from the control side. From these recorded VP

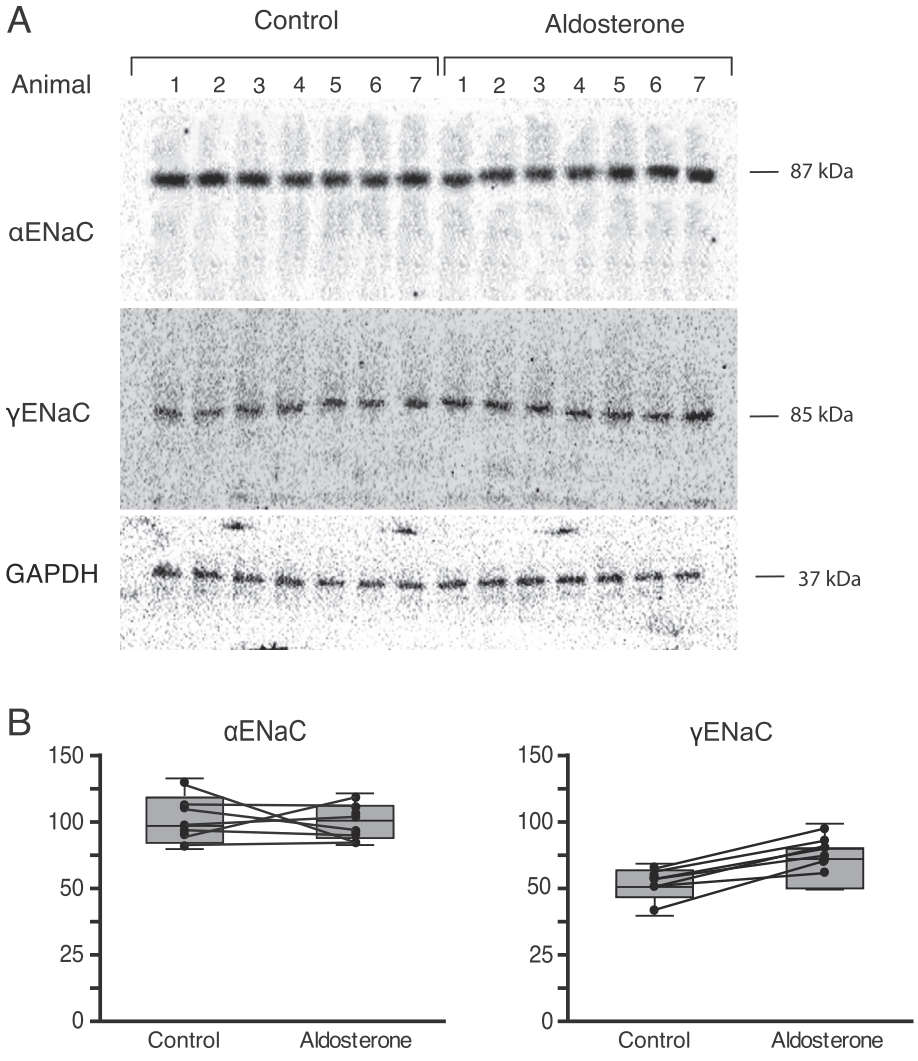

Fig. 3. The effect of aldosterone on ENaC subunit proteins abundance in hypothalamic slices. (A) Immunoblots showing the effect of aldosterone on the abundance and molecular weight of each ENaC subunit in the hypothalamic slices from 7 different animals. For each blot, each lane was loaded with the protein extract from a side of hypothalamic slices from an individual animal. The first seven lanes represent the side of the hypothalamic slice that were treated only with vehicle, whereas the following seven lanes represent the corresponding other side of slices that were treated with aldosterone. Antibodies against αENaC, γENaC, and GAPDH detected a single band at the correct molecular mass at approximately 87, 85, and 37 kDa, respectively: however, no detectable band was labeled with βENaC antibody in the protein extract from the hypothalamus. (B) Densitometric measurements of each band of αENaC and γENaC immunoblot from the side of hypothalamic slice that were treated with aldosterone and the other side of hypothalamic slices that were treated with vehicle only. A line connects data points from the same animal. The treatment with aldosterone resulted in no change in the band density of αENaC immunoblot; however, caused a significant increase in the density of γENaC immunoblot.

neurons, 12 (48%) recorded neurons from the aldosterone-treated sides and 6 (30%) recorded neurons in the control sides showed a decrease (> 2.5 pA) in the steady-state inward current held at −80 mV in response to the application of benzamil (Fig. 8A). The benzamil-sensitive current was obtained from the difference in the steady-state currents before and after the application of benzamil. The mean benzamil-sensitive current was similar in VP neurons from both the aldosterone-treated (13.1 ± 3.8nA) and control (11.7 ± 5.4 nA: Fig. 8B) sides. The effect of aldosterone on cell size was assessed by measuring the membrane capacitance of the recorded neurons. The mean whole-cell membrane capacitance did not differ between the aldosterone-treated (27.79 ± 2.55 pF) and control (23.02 ± 2.41 pF) sides, indicating that a hypertrophy of VP neurons did not occur in response to the aldosterone exposure (P = 0.252; Fig. 8B). Subsequently, the benzamil-sensitive current was normalized by the whole-cell capacitance, and the current density (pA/pF) was obtained. The mean current density (0.47 ± 0.16 nA/pF) of VP neurons from the aldosterone-treated hypothalamic slices did not differ from that (0.57 ± 0.18 nA/pF: Fig. 8C) of VP neurons from the control hypothalamic slices.

DISCUSSION

Aldosterone directly induced the expression of γENaC via MR in VP neurons

The present study demonstrated that incubation of hypothalamic slices with aldosterone resulted in induction of γENaC subunit expression, whereas αENaC and βENaC subunit expression remained at basal levels. Antagonism of the MR attenuated the effect of aldosterone on γENaC expression, indicating that aldosterone induced γENaC genomic change via the MR in the hypothalamic slices. Moreover, the result from our ChIP experiment indicated that the aldosterone–MR complex directly interacts with the hormone responding element on the γENaC gene. Because the structures that express ENaC were found only in magnocellular neurons in the PVN and SON in the hypothalamic slices used in this study and because γENaC immunoreactivity was identified prominently in the VP neurons in the SON and PVN in our previous study (Teruyama et al., 2012), the aldosterone–MR mediated regulation of γENaC expression most likely occurred specifically in VP neurons.

Corticosterone induces the expression of γENaC via GR in VP neurons

Another major finding of the present study is that corticosterone incubation resulted in a significant

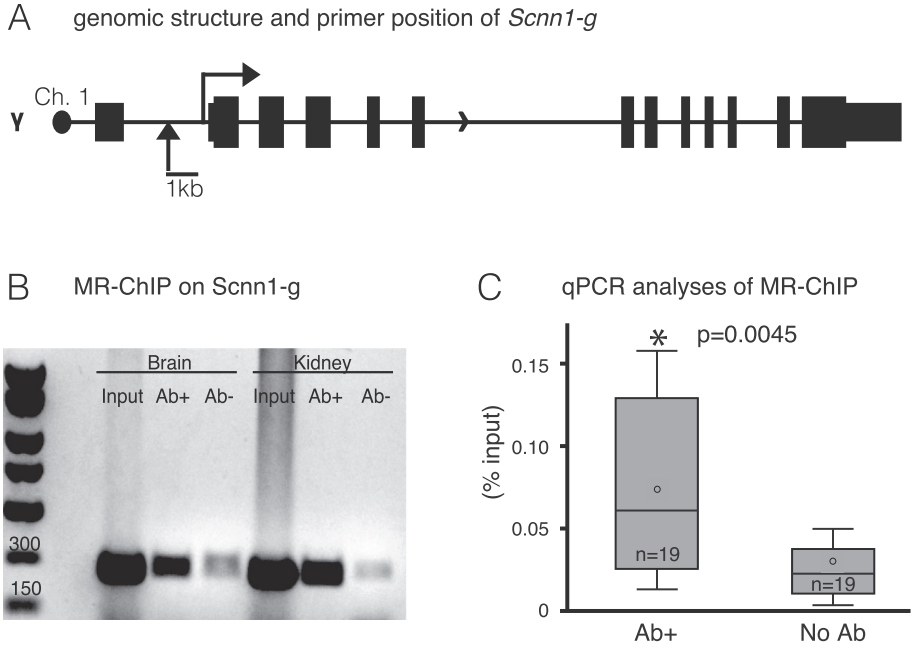

Fig. 4. Chromatin Immunoprecipitation (ChIP) with MR antibody. (A) Schematic representation of the genomic structure of *Scnn1-g* and the relative position of the primer set used for ChIP experiments. The 13 exons of *Scnn1-g* are indicated with vertical lines and boxes. B. Gel image of MR-ChIP experiment using chromatins prepared from hypothalamic region of a rat brain and kidney. The DNA from input control (n = 19), immunoprecipitates with anti-MR antibody (Ab+, n = 19), and negative controls (Ab-, n = 19) were used for PCR amplification. C. The relative amount of immunoprecipitated DNA from Ab^- and Ab^+ was further analyzed with qPCR. Shown are the relative values of the immunoprecipitates compared to the input control.

increase in γENaC expression, similar to the expressional changes observed subsequent to aldosterone incubation. Because corticosterone binds to both the GR and MR with similar affinity (Beaumont and Fanestil, 1983; Krozowski and Funder, 1983; Reul and de Kloet, 1985; Sheppard and Funder, 1987a; Sheppard and Funder, 1987b; Funder, 1995), antagonists for MR and GR were used to elucidate which receptor was activated to induce the γENaC expression. Antagonism of the MR was unable to prevent this effect of corticosterone on γENaC expression; however, an antagonist of the GR did attenuate induction of γENaC expression in the presence of corticosterone. These results indicate that corticosterone preferentially binds to the GR rather than to the MR in VP neurons to induce γENaC expression.

Although plasma concentrations of glucocorticoids are substantially higher than those of aldosterone (Holbrook et al., 1980), aldosterone is known to preferentially bind to the MR in aldosterone-sensitive epithelia (Odermatt et al., 2001). Aldosterone selectivity of the MR in the epithelia is achieved by inactivating intracellular glucocorticoids through the glucocorticoid-inactivating enzyme, 11β-hydroxysteriod dehydrogenase type 2 (11β-HSD2) (Gomez-Sanchez et al., 2005a), which converts corticosterone into inactive metabolites (Funder, 1995; Naray-Fejes-Toth et al., 1998). Thus, our present observation may be explained by our previous finding that 11β-HSD2 is expressed in the MR-expressing neurons in the SON and PVN (Haque et al., 2015).

Regulation of γENaC in VP neurons by aldosterone and corticosterone

Both the MR and GR belong to the nuclear receptor super family that act as transcription factors regulating gene expression (Vallon et al., 2005; Ronzaud et al., 2007; Ackermann et al., 2010). Upon hormone binding in the cytosol, the MR forms homodimers and heterodimers with the GR and is translocated into the nucleus where it binds to the hormone-responsive element of the target gene (Ou et al., 2001; Gekle et al., 2014). Since the DNA-binding domains of the MR and GR share approximately 94% amino acid homology (Viengchareun et al., 2007), both the MR and GR are thought to bind the common hormone-responsive elements in a sequence-specific manner to regulate some of the same genes (Evans and Arriza, 1989). The present finding that corticosterone–GR induced γENaC expression in a manner similar to that of aldosterone–MR in the hypothalamus may be due to the activation of common hormone-responsive elements on *γENaC* by the GR and MR.

Aldosterone alone does not cause increase in ENaC activity in VP neurons

Our recent study showed that the enhanced ENaC activity in response to high dietary salt intake was associated with an increase in the expression of both βENaC and γENaC subunits in the SON and the translocation of ENaC toward the plasma membrane (Sharma et al., 2017). These changes in the expression of the βENaC or the subcellular translocation of ENaC were not observed in the hypothalamic slices exposed to aldosterone *in vitro*. Therefore, other factors involved in induction of βENaC and translocation of ENaC to fully activate ENaC in VP neurons were not activated in the hypothalamic slices in media with aldosterone.

VP is known to induce the expression of βENaC subunits in the kidney (Djelidi et al., 1997; Ecelbarger et al., 2000; Nicco et al., 2001; Sauter et al., 2006). Of the three characterized VP receptor subtypes (V1a, V1b, and V2), VP appears to act through the V2 VP receptor to induce gene expression of βENaC (Nicco et al., 2001) in the kidney. VP also stimulates the translocation of intracellular pools of pre-existing ENaC subunits to the apical membrane of the principal cells in the collecting duct promoting Na^+ reabsorption in the kidney (Schafer and Hawk, 1992). VP neurons not only secrete VP at nerve terminals in the neurohypophysis, but also

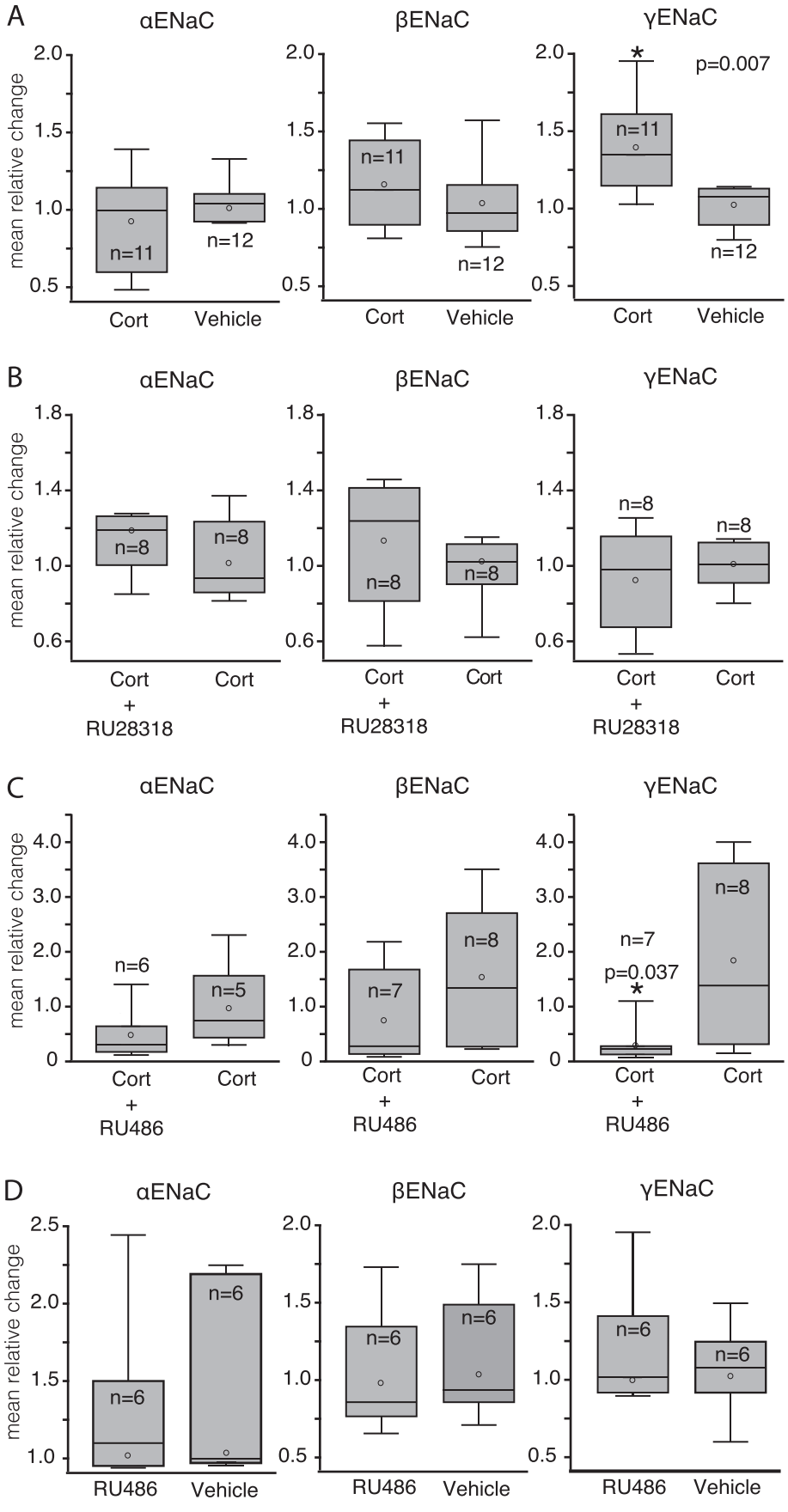

release VP from their soma and dendrites in the extracellular space of the SON and PVN (Landgraf and Ludwig, 1991; Neumann et al., 1993; Ludwig, 1998). The presence of V2 receptors on VP neurons suggests the possibility that βENaC in VP neurons could be regulated by the somato-dendritic release of VP by mechanisms similar to their regulation in the nephron. Thus, the absence of VP in the incubation media in this study may be the reason for the lack of a change in βENaC expression and translocation of ENaC in VP neurons.

Effect of aldosterone on ENaC in the brain in vivo

Our recent study (Sharma et al., 2017) found that a NaCl-deficient diet, which is known to cause an increase in aldosterone in the general circulation (Frindt et al., 1990; Pacha et al., 1993; Asher et al., 1996), did not cause a change in ENaC expression in the SON. However, the NaCl-deficient diet

Fig. 5. The effect of corticosterone on ENaC subunit expression in hypothalamic slices. (A) No significant differences in the relative amounts of αENaC and βENaC subunit mRNAs occurred between the respective sides of the hypothalamic slices that were incubated with and without corticosterone, respectively; however, the sides that were incubated with corticosterone had a significantly higher γENaC subunit expression compared to those sides incubated with vehicle only ($^{*}p < 0.007$). (B) No significant differences in αENaC, βENaC, or γENaC subunit expression occurred between the sides of the hypothalamic slices that were pre-incubated with and without MR antagonist, RU-28318, respectively. (C) No differences in αENaC and βENaC subunit expression occurred between the hypothalamic slices that were pre-incubated with and without GR antagonist, RU486, respectively; however, the hypothalamic slices that were not pre-incubated with RU486 had a significantly higher γENaC subunit expression compared to those pre-incubated with RU486 ($^{**}p < 0.037$). (D) No significant differences in αENaC, βENaC, or γENaC subunit expression observed between the sides of the hypothalamic slices that were incubated with and without RU486.

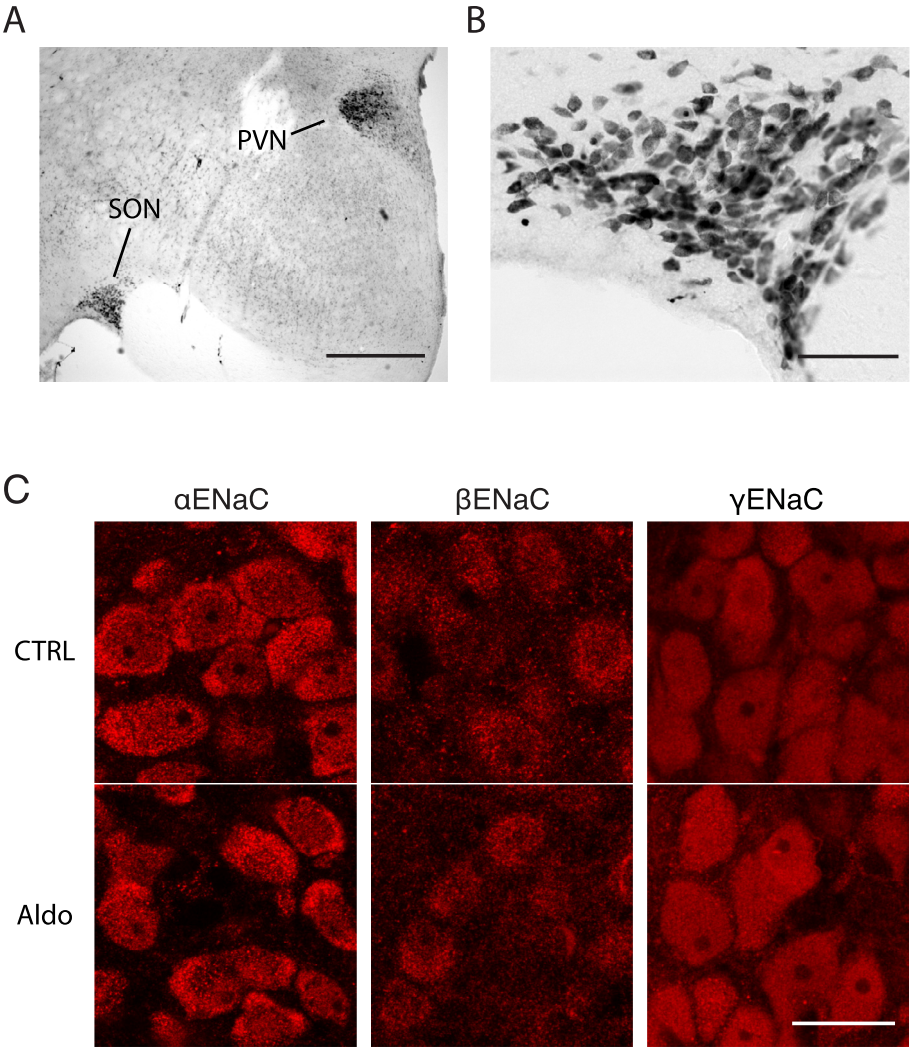

Fig. 6. Immunocytochemical localization of γENaC in the hypothalamic slices. (A) Immunoreactivity to γENaC was exclusively found in the magnocellular neurons in both the SON and PVN. Although a limited number of neurons located in the area between the SON and PVN were also immunoreactive to γENaC; no other prominent immunoreactivity was found within the hypothalamic slices. (B) In the SON, immunoreactivity to γENaC was exclusively found in the magnocellular neurons. (C) Confocal microscopy of αENaC, βENaC, and γENaC immunoreactivities in magnocellular neurons in the SON from hypothalamic slices that were treated with aldosterone (bottom panels) and vehicle only (CTRL; top panels). The αENaC immunolabeling within neurons was moderately concentrated toward the plasma membrane; no noticeable differences in subcellular distribution of αENaC immunoreactivity occurred between control and aldosterone-treated hypothalamic slices. Weak but prominent immunoreactivity of βENaC was observed in the cytoplasm. Intense γENaC immunoreactivity fully filled the cytoplasm of NaCl-deficient and control groups are mainly dispersed in the cytoplasm. No noticeable differences in subcellular distribution of βENaC or γENaC immunoreactivity occurred between control and aldosterone-treated hypothalamic slices. 1 μm optical section. Scale bars: 500 μm in A; 100 μm in B; and 50 μm in C.

did cause an increase in αENaC mRNA in the kidney known to occur in response to elevated aldosterone caused by such a diet (Renard et al., 1995; Asher et al., 1996; Escoubet et al., 1997; Stokes and Sigmund, 1998; Masilamani et al., 1999; MacDonald et al., 2000). Instead, a high-NaCl diet, which is known to decrease circulating aldosterone, caused an increase in βENaC and γENaC mRNAs in the SON (Sharma et al., 2017). This finding implies that plasma aldosterone has no effect on ENaC expression in VP neurons. Despite the lipophilicity of steroids, aldosterone is known to have a surprisingly poor penetration of the blood–brain barrier (BBB) (Pardridge and Mietus, 1979; Funder and Myles, 1996; Parker et al., 2006). This also agrees with the finding in rats that subcutaneous infusion of aldosterone increased plasma aldosterone level without significant changes in hypothalamic aldosterone content (Huang et al., 2010). Therefore, the induction of γENaC expression in VP neurons by plasma aldosterone *in vivo* is somewhat questionable.

One possible explanation for this is that aldosterone-MR-ENaC pathway in the brain is regulated independently of the peripheral/renal pathway. A growing body of evidence now suggests that aldosterone is synthesized in the CNS. The ability of brain tissue to synthesize aldosterone was demonstrated *in vitro* (Gomez-Sanchez et al., 2005b). Transcripts of aldosterone synthase (CYP11B2) were detected in various brain regions including the hypothalamus (MacKenzie et al., 2000). The presence of aldosterone synthase was detected by *in situ* hybridization in magnocellular neurons in the SON (Wang et al., 2016). Together with the present finding that γENaC in the hypothalamus is induced by aldosterone, these findings suggest that the expression of γENaC in VP neurons is regulated by aldosterone that is synthesized locally.

Our previous studies demonstrated that high dietary salt intake caused an increase in expression of γENaC in the SON of normotensive Wistar rats (Sharma et al., 2017) and in the hypothalamus of salt-sensitive Dahl rats (Mills et al., 2018). If the increased expression of γENaC is facilitated by local aldosterone, the high dietary salt intake must affect the synthesis of aldosterone in the hypothalamus. Interestingly, ICV infusion of Na^+-rich ACSF caused in rats an increase in hypothalamic aldosterone concentration and blood pressure, and both were prevented by ICV infusion of an aldosterone synthase inhibitor (Huang et al., 2008). These findings indicate that aldosterone synthesis in the hypothalamus is affected by the concentration of Na^+ in the CSF. Because the concentration of Na^+ in the CSF increased due to high dietary salt intake in salt-sensitive Dahl and spontaneously hypertensive (SHR) rats

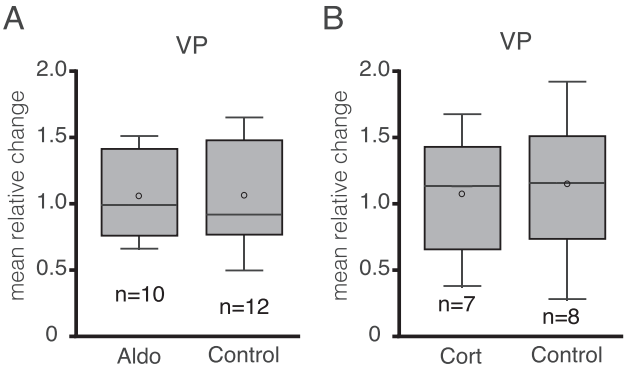

Fig. 7. The effect of corticosteroids on VP expressions in hypothalamic slices. (A) No significant differences occurred in the relative amounts of VP mRNA identified between the aldosterone- and vehicle-only incubated sides of the hypothalamic slices. (B) No significant differences occurred in the relative amounts of VP mRNA identified between the sides of hypothalamic slices that were incubated with and without corticosterone.

(Huang et al., 2004), it is possible that the elevated expression of γENaC in the hypothalamus of salt-sensitive Dahl rats that consumed high dietary salt (Mills et al., 2018) was mediated by an increased hypothalamic aldosterone production. However, the same study did not find change in CSF Na^+ concentration in normotensive salt-resistance Dahl and Wistar Kyoto rats in response to high dietary salt intake (Huang et al., 2004). Thus, it is somewhat questionable that the high dietary salt intake induced γENaC expression in the SON of normotensive Wistar rats (Sharma et al., 2017) was mediated by an increased local aldosterone synthesis that was upregulated by the increased CSF Na^+ concentration. Regardless of the change in the CSF Na^+ concentration, the aldosterone induced γENaC expression in the hypothalamus indicates that dietary salt intake influences the synthesis of aldosterone in normotensive rats as well. More research needs to be conducted to elucidate the mechanism underlying the regulation of hypothalamic aldosterone production in response to physiological demand.

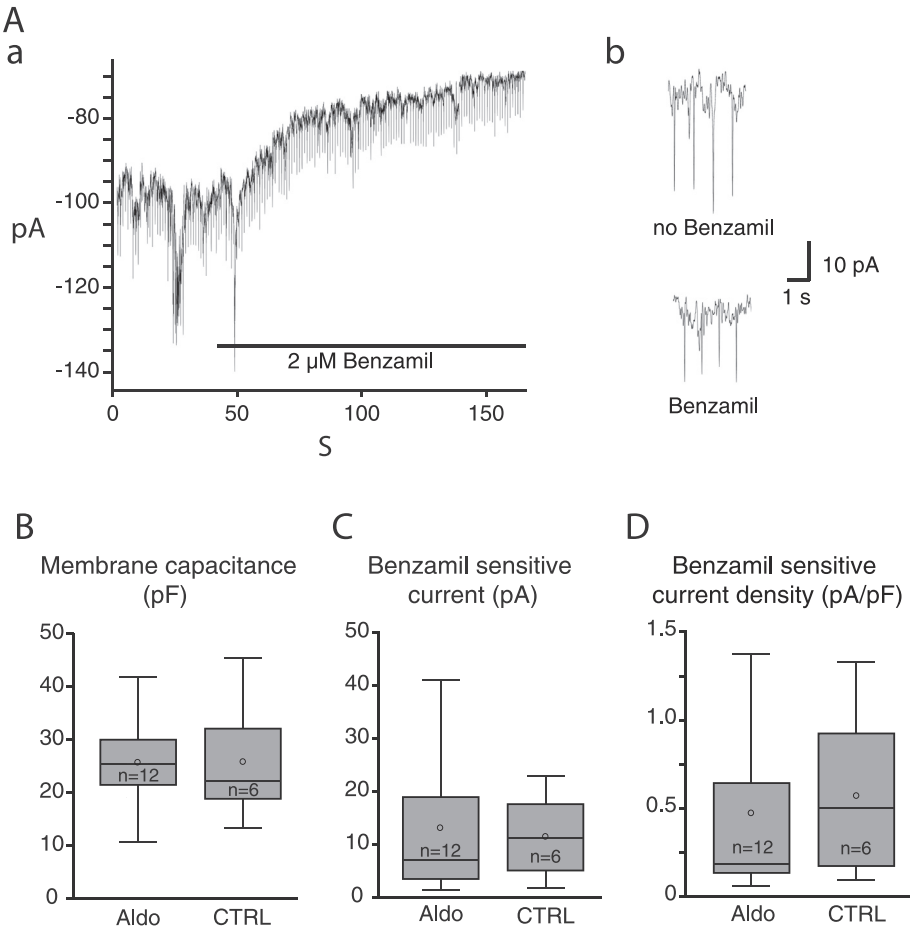

Fig. 8. The effect of aldosterone on benzamil-sensitive current. (A) An example of the effect of benzamil on the steady-state current in a VP neuron. The steady-state current was measured in voltage-clamp while the cell was held at −80 mV. Ab. Brief hyperpolarizing pulses (15 mV, 200 ms) were injected every 5 s to monitor the input resistance of the cell. Bath application of benzamil (2 μM) reduced the resting inward current and decreased conductance by approximately 1.5-fold. A benzamil-sensitive current was obtained by changes in the steady-state current in response to its application. (B) The mean benzamil-sensitive current did not differ in VP neurons from the aldosterone-treated and control sides. (C) The mean whole-cell membrane capacitance of VP neurons did not differ between the aldosterone-treated side and that from the control sides. (D) There was no difference in the mean benzamil-sensitive current density in VP neurons between the aldosterone-treated side and control sides.

Limitations of this study

The physiological plasma concentration of aldosterone (< 0.1 μM) did not induce gene expression of ENaC subunits in *in vitro* hypothalamic slices. The concentration of aldosterone used in this study was supra-physiological. For humans, this aldosterone concentration in plasma would be above the pathological range (Mattsson and Young, 2006). The supra-physiological dose was probably required for aldosterone to penetrate the relatively thick 500-μm hypothalamic slices without a functional vascular system. One of the concerns for using a supra-physiological concentration of corticosteroids is that these steroids may bind to other steroid receptors at that concentration. However, the effects of aldosterone and corticosterone on γENaC expression were attenuated by both MR and GR antagonists, respectively. In addition, the effect of corticosterone on γENaC expression was not attenuated by a MR antagonist, suggesting that the high concentration of the MR antagonist did not affect off-target receptors. Considering the presence of MRs in VP neurons (Teruyama et al., 2012; Haque et al., 2015) and the direct interaction of MR with the hormone-responding element on the γENaC gene in the SON

demonstrated by the present ChIP experiment, it is reasonable to interpret that aldosterone induces the expression of γENaC in VP neurons.

Physiological relevance and conclusion

Several *in vivo* studies suggest that ENaC in the brain are activated by aldosterone. In normotensive rats, ICV infusion of aldosterone increases blood pressure (Wang and Leenen, 2002, 2003). In salt-sensitive Dahl rats, high-salt diet or ICV infusion of aldosterone causes hypertension, but ICV infusion of a MR antagonist prevents the development of hypertension (Gomez-Sanchez et al., 1992). Intriguingly, ICV infusion of amiloride or benzamil prevents salt-induced hypertension in salt-sensitive Dahl rats (Gomez-Sanchez and Gomez-Sanchez, 1994; Wang and Leenen, 2002), as well as the hypertension induced by ICV infusion of aldosterone in normal rats (Gomez-Sanchez and Gomez-Sanchez, 1995). These findings suggest that aldosterone-mediated ENaC activation in the brain is involved in the regulation of blood pressure.

ENaC subunits and MR in the brain are colocalized only in limited regions, namely the SON, PVN, subfornical organ, choroid plexus, and ependyma of the anteroventral third ventricle (Amin et al., 2005; Teruyama et al., 2012; Haque et al., 2015). In these brain structures, VP neurons in the PVN and SON are the only structures that directly stimulate both endocrine and autonomic responses to maintain cardiovascular homeostasis. In addition to the well-characterized endocrine role of VP on antidiuretic and pressor effects, the somatodendritic release of VP stimulates the activity of parvocellular neurons that project to the rostral ventrolateral medulla (Son and Stern, 2011), thereby leading to increase in both sympathetic outflow and blood pressure (Dampney, 1994).

ENaC in VP neurons mediate a steady-state Na^+ leak current that regulates the basal membrane potential (Teruyama et al., 2012; Sharma et al., 2017). More depolarized basal membrane potential observed in VP neurons in response to high dietary salt intake was caused by increased ENaC expression and activity (Sharma et al., 2017). Therefore, activation of ENaC raises the basal membrane potential closer to the action potential threshold and consequently augments synaptic drive. Because the release of VP regulated largely by the frequency and pattern of action potential firing in their synthesizing neurons (Poulain and Wakerley, 1982; Cazalis et al., 1985), ENaC activity in VP neurons could directly influence the release of VP and autonomic responses. Thus, the physiological conditions that require VP, such as an excess dietary salt intake, may promote release of VP through ENaC activation.

The present study identified a direct involvement of aldosterone and corticosterone on γENaC expression in VP neurons via the MR and GR, respectively. Thus, aldosterone and corticosterone are likely involved in activation of ENaC in VP neurons. However, aldosterone itself is not sufficient to induce activation of ENaC in VP neurons, as neither induction of βENaC subunits nor translocation of ENaC to the plasma membrane were observed after incubation with aldosterone. Therefore, the mechanism underlying the regulation of ENaC activity in VP neurons remains largely unknown.

ACKNOWLEDGMENTS

We thank Dr. J.T. Caprio for reading earlier versions of this manuscript and Katie Huang, Richard Guidry, and Ella Baus for their excellent technical assistances.

This study was supported by National Heart, Lung, and Blood Institute Grant R01 HL115208 (Teruyama).

This work was supported in part from a grant to the Louisiana State University College of Science from the NIH Bridges to the Baccalaureate Program.

REFERENCES

Ackermann D, Gresko N, Carrel M, Loffing-Cueni D, Habermehl D, Gomez-Sanchez C, Rossier BC, Loffing J (2010) In vivo nuclear translocation of mineralocorticoid and glucocorticoid receptors in rat kidney: differential effect of corticosteroids along the distal tubule. Am J Physiol Renal Physiol 299:F1473–F1485.

Amin MS, Reza E, Wang H, Leenen FH (2009) Sodium transport in the choroid plexus and salt-sensitive hypertension. Hypertension 54:860–867.

Amin MS, Wang HW, Reza E, Whitman SC, Tuana BS, Leenen FH (2005) Distribution of epithelial sodium channels and mineralocorticoid receptors in cardiovascular regulatory centers in rat brain. Am J Physiol Regul Integr Comp Physiol 289: R1787–R1797.

Asher C, Wald H, Rossier BC, Garty H (1996) Aldosterone-induced increase in the abundance of Na+ channel subunits. Am J Physiol 271:C605–C611.

Beaumont K, Fanestil DD (1983) Characterization of rat brain aldosterone receptors reveals high affinity for corticosterone. Endocrinology 113:2043–2051.

Brimble MJ, Dyball RE (1977) Characterization of the responses of oxytocin- and vasopressin-secreting neurones in the supraoptic nucleus to osmotic stimulation. J Physiol 271:253–271.

Canessa CM, Schild L, Buell G, Thorens B, Gautschi I, Horisberger JD, Rossier BC (1994) Amiloride-sensitive epithelial Na+ channel is made of three homologous subunits. Nature 367:463–467.

Cazalis M, Dayanithi G, Nordmann JJ (1985) The role of patterned burst and interburst interval on the excitation-coupling mechanism in the isolated rat neural lobe. J Physiol 369:45–60.

Dampney RA (1994) Functional organization of central pathways regulating the cardiovascular system. Physiol Rev 74:323–364.

Djelidi S, Fay M, Cluzeaud F, Escoubet B, Eugene E, Capurro C, Bonvalet JP, Farman N, Blot-Chabaud M (1997) Transcriptional regulation of sodium transport by vasopressin in renal cells. J Biol Chem 272:32919–32924.

Ecelbarger CA, Kim GH, Terris J, Masilamani S, Mitchell C, Reyes I, Verbalis JG, Knepper MA (2000) Vasopressin-mediated regulation of epithelial sodium channel abundance in rat kidney. Am J Physiol Renal Physiol 279:F46–F53.

Escoubet B, Coureau C, Bonvalet JP, Farman N (1997) Noncoordinate regulation of epithelial Na channel and Na pump subunit mRNAs in kidney and colon by aldosterone. Am J Physiol 272:C1482–C1491.

Evans RM, Arriza JL (1989) A molecular framework for the actions of glucocorticoid hormones in the nervous system. Neuron 2:1105–1112.

Frindt G, Sackin H, Palmer LG (1990) Whole-cell currents in rat cortical collecting tubule: low-Na diet increases amiloride-sensitive conductance. Am J Physiol 258:F562–F567.

Funder J, Myles K (1996) Exclusion of corticosterone from epithelial mineralocorticoid receptors is insufficient for selectivity of aldosterone action: in vivo binding studies. Endocrinology 137:5264–5268.
Funder JW (1995) The promiscuous receptor: a case for the guardian enzyme. Cardiovasc Res 30:177–180.
Geerling JC, Loewy AD (2009) Aldosterone in the brain. Am J Physiol Renal Physiol 297:F559–F576.
Gekle M, Bretschneider M, Meinel S, Ruhs S, Grossmann C (2014) Rapid mineralocorticoid receptor trafficking. Steroids 81:103–108.
Gomez-Sanchez EP, Gomez-Sanchez CE (1994) Effect of central amiloride infusion on mineralocorticoid hypertension. Am J Physiol 267:E754–E758.
Gomez-Sanchez EP, Gomez-Sanchez CE (1995) Effect of central infusion of benzamil on Dahl S rat hypertension. Am J Physiol 269:H1044–H1047.
Gomez-Sanchez EP, Fort C, Thwaites D (1992) Central mineralocorticoid receptor antagonism blocks hypertension in Dahl S/JR rats. Am J Physiol 262:E96–E99.
Gomez-Sanchez EP, Samuel J, Vergara G, Ahmad N (2005a) Effect of 3beta-hydroxysteroid dehydrogenase inhibition by trilostane on blood pressure in the Dahl salt-sensitive rat. Am J Physiol Regul Integr Comp Physiol 288:R389–R393.
Gomez-Sanchez EP, Ahmad N, Romero DG, Gomez-Sanchez CE (2005b) Is aldosterone synthesized within the rat brain? Am J Physiol Endocrinol Metab 288:E342–E346.
Han F, Ozawa H, Matsuda K, Nishi M, Kawata M (2005) Colocalization of mineralocorticoid receptor and glucocorticoid receptor in the hippocampus and hypothalamus. Neurosci Res 51:371–381.
Haque M, Wilson R, Sharma K, Mills NJ, Teruyama R (2015) Localisation of 11beta-hydroxysteroid dehydrogenase type 2 in mineralocorticoid receptor expressing magnocellular neurosecretory neurones of the rat supraoptic and paraventricular nuclei. J Neuroendocrinol 27:835–849.
Harris MC, Dreifuss JJ, Legros JJ (1975) Excitation of phasically firing supraoptic neurones during vasopressin release. Nature 258:80–82.
Holbrook MM, Dale SL, Melby JC (1980) Peripheral plasma steroid concentrations in rats sacrificed by anoxia. J Steroid Biochem 13:1355–1358.
Huang BS, Van Vliet BN, Leenen FH (2004) Increases in CSF [Na+] precede the increases in blood pressure in Dahl S rats and SHR on a high-salt diet. Am J Physiol Heart Circ Physiol 287: H1160–H1166.
Huang BS, White RA, Ahmad M, Jeng AY, Leenen FH (2008) Central infusion of aldosterone synthase inhibitor prevents sympathetic hyperactivity and hypertension by central Na+ in Wistar rats. Am J Physiol Regul Integr Comp Physiol 295:R166–R172.
Huang BS, Ahmadi S, Ahmad M, White RA, Leenen FH (2010) Central neuronal activation and pressor responses induced by circulating ANG II: role of the brain aldosterone-‘‘ouabain” pathway. Am J Physiol Heart Circ Physiol 299:H422–H430.
Ito K, Hirooka Y, Sunagawa K (2015) Cardiac sympathetic afferent stimulation induces salt-sensitive sympathoexcitation through hypothalamic epithelial Na+ channel activation. Am J Physiol Heart Circ Physiol 308:H530–H539.
Janiak P, Brody MJ (1988) Central interactions between aldosterone and vasopressin on cardiovascular system. Am J Physiol 255: R166–R173.
Keep RF, Si X, Shakui P, Ennis SR, Betz AL (1999) Effect of amiloride analogs on DOCA-salt-induced hypertension in rats. Am J Physiol 276:H2215–H2220.
Khanna S, Sibbald JR, Smith DW, Day TA (1994) Initiation of rat vasopressin cell responses to simulated hypotensive hemorrhage. Am J Physiol 267:R1142.
Kleyman TR, Cragoe Jr EJ (1988) Amiloride and its analogs as tools in the study of ion transport. J Membr Biol 105:1–21.
Krozowski ZS, Funder JW (1983) Renal mineralocorticoid receptors and hippocampal corticosterone-binding species have identical intrinsic steroid specificity. Proc Natl Acad Sci U S A 80:6056–6060.
Landgraf R, Ludwig M (1991) Vasopressin release within the supraoptic and paraventricular nuclei of the rat brain: osmotic stimulation via microdialysis. Brain Res 558:191–196.
Ludwig M (1998) Dendritic release of vasopressin and oxytocin. J Neuroendocrinol 10:881–895.
MacDonald P, MacKenzie S, Ramage LE, Seckl JR, Brown RW (2000) Corticosteroid regulation of amiloride-sensitive sodium-channel subunit mRNA expression in mouse kidney. J Endocrinol 165:25–37.
MacKenzie SM, Clark CJ, Fraser R, Gomez-Sanchez CE, Connell JM, Davies E (2000) Expression of 11beta-hydroxylase and aldosterone synthase genes in the rat brain. J Mol Endocrinol 24:321–328.
Masilamani S, Kim GH, Mitchell C, Wade JB, Knepper MA (1999) Aldosterone-mediated regulation of ENaC alpha, beta, and gamma subunit proteins in rat kidney. J Clin Invest 104:R19–R23.
Mattsson C, Young Jr WF (2006) Primary aldosteronism: diagnostic and treatment strategies. Nat Clin Pract Nephrol 2:198–208. quiz, 191 p following 230.
Miller RL, Loewy AD (2013) ENaC gamma-expressing astrocytes in the circumventricular organs, white matter, and ventral medullary surface: sites for Na+ regulation by glial cells. J Chem Neuroanat 53:72–80.
Miller RL, Wang MH, Gray PA, Salkoff LB, Loewy AD (2013) ENaC-expressing neurons in the sensory circumventricular organs become c-Fos activated following systemic sodium changes. Am J Physiol Regul Integr Comp Physiol 305:R1141–R1152.
Mills NJ, Sharma K, Huang K, Teruyama R (2018) Effect of dietary salt intake on epithelial Na+ channels (ENaCs) in the hypothalamus of Dahl salt-sensitive rats. Physiol Rep. Manuscript Accepted.
Naray-Fejes-Toth A, Colombowala IK, Fejes-Toth G (1998) The role of 11beta-hydroxysteroid dehydrogenase in steroid hormone specificity. J Steroid Biochem Mol Biol 65:311–316.
Neumann I, Russell JA, Landgraf R (1993) Oxytocin and vasopressin release within the supraoptic and paraventricular nuclei of pregnant, parturient and lactating rats: a microdialysis study. Neuroscience 53:65–75.
Nicco C, Wittner M, DiStefano A, Jounier S, Bankir L, Bouby N (2001) Chronic exposure to vasopressin upregulates ENaC and sodium transport in the rat renal collecting duct and lung. Hypertension 38:1143–1149.
Nishimura M, Ohtsuka K, Nanbu A, Takahashi H, Yoshimura M (1998) Benzamil blockade of brain Na+ channels averts Na(+)-induced hypertension in rats. Am J Physiol 274:R635–R644.
Nishimura M, Ohtsuka K, Iwai N, Takahashi H, Yoshimura M (1999) Regulation of brain renin-angiotensin system by benzamil-blockable sodium channels. Am J Physiol 276: R1416–R1424.
Odermatt A, Arnold P, Frey FJ (2001) The intracellular localization of the mineralocorticoid receptor is regulated by 11beta-hydroxysteroid dehydrogenase type 2. J Biol Chem 276:28484–28492.
Oliet SH, Bourque CW (1993) Mechanosensitive channels transduce osmosensitivity in supraoptic neurons. Nature 364:341–343.
Ou XM, Storring JM, Kushwaha N, Albert PR (2001) Heterodimerization of mineralocorticoid and glucocorticoid receptors at a novel negative response element of the 5-HT1A receptor gene. J Biol Chem 276:14299–14307.
Pacha J, Frindt G, Antonian L, Silver RB, Palmer LG (1993) Regulation of Na channels of the rat cortical collecting tubule by aldosterone. J Gen Physiol 102:25–42.
Pardridge WM, Mietus LJ (1979) Transport of steroid hormones through the rat blood-brain barrier. Primary role of albumin-bound hormone. The J Clin Invest 64:145–154.
Parker RB, Yates CR, Laizure SC, Weber KT (2006) P-glycoprotein modulates aldosterone plasma disposition and tissue uptake. J Cardiovasc Pharmacol 47:55–59.

Poulain DA, Wakerley JB (1982) Electrophysiology of hypothalamic magnocellular neurones secreting oxytocin and vasopressin. Neuroscience 7:773–808.
Renard S, Voilley N, Bassilana F, Lazdunski M, Barbry P (1995) Localization and regulation by steroids of the alpha, beta and gamma subunits of the amiloride-sensitive Na + channel in colon, lung and kidney. Pflugers Arch 430:299–307.
Reul JM, de Kloet ER (1985) Two receptor systems for corticosterone in rat brain: microdistribution and differential occupation. Endocrinology 117:2505–2511.
Ronzaud C, Loffing J, Bleich M, Gretz N, Grone HJ, Schutz G, Berger S (2007) Impairment of sodium balance in mice deficient in renal principal cell mineralocorticoid receptor. J Am Soc Nephrol 18:1679–1687.
Sauter D, Fernandes S, Goncalves-Mendes N, Boulkroun S, Bankir L, Loffing J, Bouby N (2006) Long-term effects of vasopressin on the subcellular localization of ENaC in the renal collecting system. Kidney Int 69:1024–1032.
Schafer JA, Hawk CT (1992) Regulation of Na + channels in the cortical collecting duct by AVP and mineralocorticoids. Kidney Int 41:255–268.
Schreiber JR, Hsueh AJ, Baulieu EE (1983) Binding of the anti-progestin RU-486 to rat ovary steroid receptors. Contraception 28:77–85.
Sharma K, Haque M, Guidry R, Ueta Y, Teruyama R (2017) Effect of dietary salt intake on epithelial Na + channels (ENaC) in vasopressin magnocellular neurosecretory neurons in the rat supraoptic nucleus. J Physiol 595:5857–5874.
Sheppard K, Funder JW JW (1987a) Type I receptors in parotid, colon, and pituitary are aldosterone selective in vivo. Am J Physiol 253:E467–E471.
Sheppard KE, Funder JW (1987b) Equivalent affinity of aldosterone and corticosterone for type I receptors in kidney and hippocampus: direct binding studies. J Steroid Biochem 28:737–742.
Son SJ, Stern JE (2011) Activity-dependent release of vasopressin within the PVN mediate cross-talk between neuroendocrine and sympathetic-related PVN. 9th World Congress on Neurohypophysial hormones abstract.
Stokes JB, Sigmund RD (1998) Regulation of rENaC mRNA by dietary NaCl and steroids: organ, tissue, and steroid heterogeneity. Am J Physiol 274:C1699–C1707.
Teruyama R, Armstrong WE (2005) Enhancement of calcium-dependent afterpotentials in oxytocin neurons of the rat supraoptic nucleus during lactation. J Physiol 566:505–518.
Teruyama R, Armstrong WE (2007) Calcium-dependent fast depolarizing afterpotentials in vasopressin neurons in the rat supraoptic nucleus. J Neurophysiol.
Teruyama R, Sakuraba M, Wilson LL, Wandrey NE, Armstrong WE (2012) Epithelial Na(+) sodium channels in magnocellular cells of the rat supraoptic and paraventricular nuclei. Am J Physiol Endocrinol Metabol 302:E273–E285.
Vallon V, Huang DY, Grahammer F, Wyatt AW, Osswald H, Wulff P, Kuhl D, Lang F (2005) SGK1 as a determinant of kidney function and salt intake in response to mineralocorticoid excess. Am J Physiol Regul Integr Comp Physiol 289:R395–R401.
van Eekelen JA, Bohn MC, de Kloet ER (1991) Postnatal ontogeny of mineralocorticoid and glucocorticoid receptor gene expression in regions of the rat tel- and diencephalon. Brain Res Dev Brain Res 61:33–43.
Viengchareun S, Le Menuet D, Martinerie L, Munier M, Pascual-Le Tallec L, Lombes M (2007) The mineralocorticoid receptor: insights into its molecular and (patho)physiological biology. Nucl Recept Signal 5 e012.
Wang H, Leenen FH (2002) Brain sodium channels mediate increases in brain ‘‘ouabain” and blood pressure in Dahl S rats. Hypertension 40:96–100.
Wang H, Leenen FH (2003) Brain sodium channels and central sodium-induced increases in brain ouabain-like compound and blood pressure. J Hypertens 21:1519–1524.
Wang H, Huang BS, Leenen FH (2003) Brain sodium channels and ouabainlike compounds mediate central aldosterone-induced hypertension. Am J Physiol Heart Circ Physiol 285:H2516–2523.
Wang HW, Huang BS, Chen A, Ahmad M, White RA, Leenen FH (2016) Role of brain aldosterone and mineralocorticoid receptors in aldosterone-salt hypertension in rats. Neuroscience 314:90–105.

(Received 7 December 2017, Accepted 28 August 2018)
(Available online 6 September 2018)